Available online at www.sciencedirect.com
SCIENCE DIRECT
Catalysis Today 112 (2006) 53–59
CATALYSIS TODAY
www.elsevier.com/locate/cattod

Kinetic modelling of the gas phase ethane and propane oxidative dehydrogenation

M. Machli [a], C. Boudouris [a], S. Gaab [b], J. Find [b], A.A. Lemonidou [a,*], J.A. Lercher [b]

[a] *Department of Chemical Engineering, Aristotle University of Thessaloniki and Chemical Process Engineering Research Institute, P.O. Box 1517, University City 54006, Thessaloniki, Greece*

[b] *Department of Chemistry, TU München, Lichtenbergstr. 4, 85747 Garching, Germany*

Available online 28 December 2005

Abstract

Gas phase thermal and oxidative dehydrogenation of ethane and propane are explored experimentally and mikrokinetically. Kinetic data for the elementary reactions postulated were adopted from the literature. The results show that oxygen plays a dominating role in the primary activation of the alkanes by producing an $HO_2^{\bullet}$ and a hydrocarbon radical. The kinetic sequences developed predict satisfactorily conversion and products yields for ethane and propane oxidative dehydrogenation.

Keywords: Kinetic modelling; Gas phase oxidative dehydrogenation; Ethane; Propane

1. Introduction

Oxidative dehydrogenation (ODH) presents a challenging but viable route for olefin production from alkanes, which may overcome drawbacks of the presently practiced processes. Ideally, the alkane reacts with oxygen to the desired olefin and water. The process requires catalysts able to activate alkanes, while preserving the formed alkenes from further oxidation to COx.

The contribution of the gas phase reactions in the catalytic oxidative dehydrogenation of alkanes is very important, especially when reaction temperatures above 600 °C are employed [1–3]. A number of studies addressing homogeneous reactions for oxidative dehydrogenation of C_2–C_4 alkanes have so far been published [4–9]. Burch and Grabb report the non-catalytic oxidative dehydrogenation of ethane to ethene in a quartz reactor to be efficient with the yield of ethene depending on the temperature and the ethane to oxygen ratio used [4]. In contrast, Mulla et al. did not observe significant reactions up to 700 °C in the absence of a catalyst using a low volume reactor [5]. On the other hand, Beretta et al. report homogeneous reactions during oxidative dehydrogenation of ethane to be important even at 600 °C [6].

While it is generally accepted that homogeneous reactions proceed via free-radical chain mechanism, none of the studies cited above provides a sufficient kinetic model describing the homogeneous gas phase oxidative dehydrogenation of lower alkanes. Therefore, the effect of the operational conditions (such as temperature, alkane–oxygen ratio in the feed, residence time) on the conversion of reactants and product yields for the gas phase oxidative dehydrogenation of ethane and propane was explored. Kinetic models comprising of elementary reactions have been developed for the simulation of the experimental data. The sets of elementary reactions used for the oxidative dehydrogenation of ethane and propane consisted of 75 and 73 individual elementary reactions, respectively. The differential equations describing the mass balance of the species in PFR reactor were solved using the Gear method.

2. Experimental

The experiments of gas phase oxidative dehydrogenation of ethane and propane were conducted in a quartz tube flow reactor (i.d. 10 mm) with a volume of 5.6 ml operating at pressures up to 1.3 bar. A thermocouple placed coaxially in the center of the reactor was used for temperature monitoring. The reactor was heated electrically and the isothermal zone of the

* Corresponding author.
E-mail address: alemonidou@cheng.auth.gr (A.A. Lemonidou).

0920-5861/$ – see front matter © 2005 Elsevier B.V. All rights reserved.
doi:10.1016/j.cattod.2005.11.027

oven coincided with the fraction of the reactor having a significant void volume. Quartz sticks were placed in the narrower parts of the reactor for minimizing the void volume. The reactant feed was introduced in the reactor by means of mass flow controllers. For the oxidative dehydrogenation of ethane, the gases used were C_2H_6 (99.9%), O_2 (10.4% in He) and for the balance He (99.99%). Runs were conducted at temperatures from 575 to 650 °C, at a constant residence time 2.4 s (calculated at reaction conditions). The ethane partial pressure was 80 mbar and that of oxygen varied from 16 to 80 mbar. Quantifiable reaction products were C_2H_4, CO, CO_2 and H_2O. Additionally, traces of hydrocarbons higher than C_2, oxygenates and H_2 were also detected. Propane oxidative dehydrogenation were conducted from 575 to 675 °C using C_3H_8 (5% in He), O_2 (99.9%) and He (99.99%). The propane and oxygen partial pressures were constant at 50 mbar. The reaction products were mainly C_3H_6, C_2H_4, CH_4, CO_2, CO and H_2O. Again, minor amounts of hydrocarbons higher than C_3, oxygenates and H_2 were also detected. Reactor effluents were analyzed by on line gas chromatography using a Pora Plot Q and a Molsieve column for product separation. The mass balance based on carbon was 100 ± 2% for all experiments.

3. Model development

For the model development isothermal operation at atmospheric pressure and plug flow conditions were assumed. Both assumptions are well justified by the high dilution and the high linear flows used. Continuity equations were written for all species, radicals and molecules. It was assumed that reactions are elementary and the rate coefficients obey the Arrhenius relationship. The kinetic parameters of the elementary reactions were adopted from literature [9–15]. For a limited number of reactions the frequency factor has been varied by ±10% in order to fit the experimental data. Reverse reactions were explicitly included. The simulations were performed using a FORTRAN program developed in our group.

In general, the program sequence starts with the introduction of the reaction data, the formation of the stoichiometric coefficients matrix for all compounds and the formation of reactions order matrix followed by the reaction conditions (temperature, pressure, reactor volume, total volumetric flow and the percentage of reactants in the feed). The system of reactions is developed by means of an FCN subroutine (IMSL) and is integrated numerically by the use of DIVPAG subroutine (IMSL), which solves non-linear ordinary differential equations using the Gear method. The program output includes the calculation of carbon, hydrogen and oxygen mass balance, alkane and oxygen conversion, as the well as the volume percentage and the yield of all products.

4. Results

4.1. Oxidative dehydrogenation of ethane

The experiments of ethane ODH in an empty reactor showed that gas phase reactions take place above 575 °C for a nominal residence time 2.4 s and equimolar alkane and oxygen flows (Fig. 1). Ethane is converted with high selectivity to ethene, while COx and especially CO are the main by-products. Conversions of ethane and oxygen increase drastically with temperature approaching 80% and 90%, respectively, at 650 °C. The yield to ethene is very high reaching 56% at 650 °C (Fig. 1). The effect of oxygen partial pressure on the reaction rates was also examined. Experiments conducted with oxygen partial pressure varying from 16 to 48 mbar and an ethane partial pressure of 80 mbar show that the conversion increases with the partial pressure of oxygen.

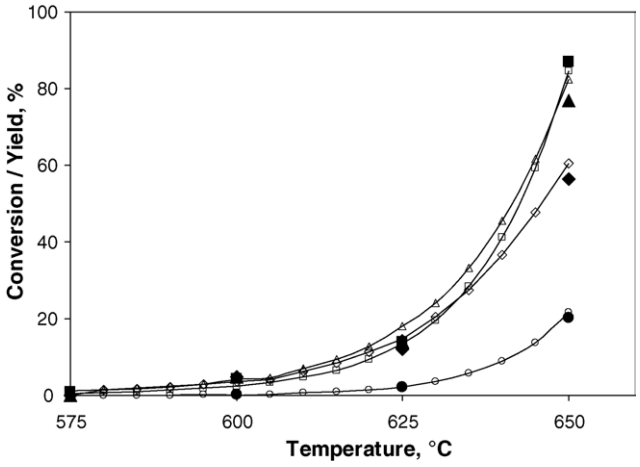

Fig. 1. Conversion and products yield vs. temperature in gas phase ethane oxidative dehydrogenation (residence time = 2.4 s, $P_{C_2H_6} = P_{O_2}$ = 80 mbar). C_2H_6: (■) experimental, (□) calculated; O_2: (▲) experimental, (△) calculated; C_2H_4: (◆) experimental, (◇) calculated; COx: (●) experimental, (○) calculated.

In establishing the reaction network the elementary reactions involving radicals were classified into several categories, i.e., (i) initiation reactions leading to the formation of free radicals, (ii) hydrogen atom abstraction reactions from hydrocarbon with or without the participation of oxygen radicals, (iii) addition reactions between a free radical and a molecular compound to generate a new free radical, (iv) decomposition reactions, (v) carbon oxides formation and (vi) termination reactions in which two radicals form one or two molecular compounds.

The reaction scheme accounted for 12 molecular compounds and 17 free radicals. The selection of the elementary reactions was based on mechanistic models of thermal pyrolysis and oxidation of ethane [10,11,13]. The sensitivity analysis to assess the significance of the each one of the initially proposed reactions to model predictions resulted in a simplified model including 75 elementary reactions.

The initiation reactions involve the reaction between ethane and molecular oxygen producing $C_2H_5^{\bullet}$ and $HO_2^{\bullet}$, as well as the pyrolysis route, converting ethane to two $CH_3^{\bullet}$ radicals. The reactions and their kinetic data are presented in Table 1. The lower activation energy of the reaction (2) suggests that oxygen is involved in the initiating reaction steps. As a consequence the oxidative dehydrogenation (reaction (2)) is favored at lower temperatures, while thermal pyrolysis at higher temperatures. It should be mentioned that oxygen is also important for the propagation reactions. $CH_3^{\bullet}$ radicals, formed at high tempera-

Table 1
Elementary reactions and kinetic data for ethane gas phase ODH [10,11,13]

	Reactions	log k_0 (s^{-1} or cm mol^{-1} s^{-1})	E (kJ/mol)
Initiation			
1	$C_2H_6 \rightarrow CH_3^{\bullet} + CH_3^{\bullet}$	12.07	284.09
2	$C_2H_6 + O_2 \rightarrow C_2H_5^{\bullet} + HO_2^{\bullet}$	14	233.47
Hydrogen atom abstraction			0.00
3	$C_2H_5^{\bullet} + H_2O_2 \rightarrow C_2H_6 + HO_2^{\bullet}$	10.93	22.59
4	$C_2H_4 + O_2 \rightarrow C_2H_3^{\bullet} + HO_2^{\bullet}$	13.6	257.32
5	$CH_4 + O_2 \rightarrow CH_3^{\bullet} + HO_2^{\bullet}$	14.6	238.07
6	$CH_2^{\bullet} + H^{\bullet} \rightarrow CH^{\bullet} + H_2$	18	−7.53
7	$C_2H_4 + H^{\bullet} \rightarrow C_2H_3^{\bullet} + H_2$	14.7	62.34
8	$C_3H_4 + H^{\bullet} \rightarrow C_3H_3^{\bullet} + H_2$	12	6.28
9	$C_4H_4 + H^{\bullet} \rightarrow C_4H_3^{\bullet} + H_2$	6.7	25.10
10	$C_2H_2O^{\bullet} + H^{\bullet} \rightarrow C_2HO^{\bullet} + H_2$	14.25	35.98
11	$C_2H_6 + CH_2^{\bullet} \rightarrow CH_3^{\bullet} + C_2H_5$	12.81	33.05
12	$C_2H_4 + CH_3^{\bullet} \rightarrow C_2H_3^{\bullet} + CH_4$	11.18	46.44
13	$C_2H_6 + CH_3^{\bullet} \rightarrow C_2H_5^{\bullet} + CH_4$	8.9	50.21
14	$C_2H_2O^{\bullet} + CH_3^{\bullet} \rightarrow C_2HO^{\bullet} + CH_4$	12.88	54.39
15	$C_2H^{\bullet} + H_2 \rightarrow C_2H_2 + H^{\bullet}$	12.3	0.00
16	$C_2H_3^{\bullet} + H_2 \rightarrow C_2H_4 + H^{\bullet}$	12.62	65.69
17	$C_2H_6 + C_2H_3^{\bullet} \rightarrow C_2H_5^{\bullet} + C_2H_4$	−1.05	10.46
18	$CH_2^{\bullet} + O^{\bullet} \rightarrow CH^{\bullet} + OH^{\bullet}$	13.7	0.00
19	$C_2H_2 + O^{\bullet} \rightarrow C_2H^{\bullet} + OH^{\bullet}$	15.49	62.76
20	$CH_2^{\bullet} + OH^{\bullet} \rightarrow CH^{\bullet}, + H_2O$	11.43	107.53
21	$CH_3^{\bullet} + OH^{\bullet} \rightarrow CH_2^{\bullet} + H_2O$	13.28	20.92
22	$CH_4 + OH^{\bullet} \rightarrow CH_3^{\bullet} + H_2O$	3.54	8.37
23	$C_2H_2 + OH^{\bullet} \rightarrow C_2H^{\bullet} + H_2O$	7.53	58.58
24	$C_2H_5^{\bullet} + OH^{\bullet} \rightarrow C_2H_6 + O^{\bullet}$	12.23	42.68
25	$CH_4 + HO_2^{\bullet} \rightarrow CH_3^{\bullet} + H_2O_2$	10.26	77.82
26	$C_2H_4 + HO_2^{\bullet} \rightarrow C_2H_5^{\bullet} + O_2$	11.87	58.58
27	$C_2H_6 + HO_2^{\bullet} \rightarrow C_2H_5^{\bullet} + H_2O_2$	11	62.34
28	$C_2H_5^{\bullet} + O_2 \rightarrow C_2H_4 + HO_2^{\bullet}$	10	−9.20
29	$C_2H_3^{\bullet} + H_2O \rightarrow C_2H_4 + OH^{\bullet}$	11.41	61.50
Addition			0.00
30	$C_2H_2 + H^{\bullet} \rightarrow C_2H_3^{\bullet}$	11.09	−43.51
31	$CH_3^{\bullet} + CH_2^{\bullet} \rightarrow C_2H_4 + H^{\bullet}$	13.6	0.00
32	$CH_3^{\bullet} + CH_3^{\bullet} \rightarrow C_2H_5^{\bullet} + H^{\bullet}$	12.18	44.35
Decomposition			0.00
33	$C_2H_3^{\bullet} \rightarrow C_2H_2 + H^{\bullet}$	14.2	158.16
34	$C_4H_3^{\bullet} \rightarrow C_2H_2 + C_2H^{\bullet}$	14.5	239.32
35	$C_4H_4^{\bullet} \rightarrow C_2H_2 + C_2H_2$	13.5	322.59
36	$C_3H_4^{\bullet} + H^{\bullet} \rightarrow C_2H_2 + CH_3^{\bullet}$	5.1	4.18
37	$H_2O_2 \rightarrow OH + OH^{\bullet}$	6	46.02
38	$H_2O_2 + O_2 \rightarrow HO_2^{\bullet} + HO_2$	13.6	178.24
Carbon oxides formation			0.00
39	$OH^{\bullet} + H_2 \rightarrow H^{\bullet} + H_2O$	9.08	14.64
40	$CH_3^{\bullet} + O_2 \rightarrow CH_3O^{\bullet} + O^{\bullet}$	13	107.11
41	$CH_3^{\bullet} + O_2 \rightarrow CH_2O + OH^{\bullet}$	10.55	144.77
42	$CH_3^{\bullet} + O^{\bullet} \rightarrow CH_2O + H^{\bullet}$	13.85	0.00
43	$CH^{\bullet} + O_2 \rightarrow CO_2 + H^{\bullet}$	13.3	0.00
44	$C_2H_2 + OH^{\bullet} \rightarrow C_2H_2O^{\bullet} + H^{\bullet}$	11.5	0.84
45	$C_2H_2 + O^{\bullet} \rightarrow C_2HO^{\bullet} + H^{\bullet}$	14.7	44.77
46	$CH_2O + O_2 \rightarrow HCO^{\bullet} + HO_2^{\bullet}$	13.78	170.29
47	$CH_2O + O^{\bullet} \rightarrow HCO^{\bullet} + OH^{\bullet}$	13.26	12.97
48	$CH_2O + OH^{\bullet} \rightarrow HCO^{\bullet} + H_2O$	13.48	38.49
49	$HCO^{\bullet} + OH^{\bullet} \rightarrow CO + H_2O$	13.7	0.00
50	$HCO^{\bullet} + O_2 \rightarrow HO_2^{\bullet} + CO$	10	0.00
51	$CO + OH^{\bullet} \rightarrow CO_2 + H^{\bullet}$	2.2	−81.17
52	$CO_2 + H^{\bullet} \rightarrow CO + OH^{\bullet}$	9.23	90.37
53	$CO_2 + OH^{\bullet} \rightarrow HO_2^{\bullet} + CO$	11.5	307.94
54	$CO + HO_2^{\bullet} \rightarrow OH^{\bullet} + CO_2$	10.17	100.42
55	$CO_2 + O^{\bullet} \rightarrow CO + O_2$	12.44	183.26
56	$CO + O_2 \rightarrow CO_2 + O^{\bullet}$	11.5	307.94
57	$C_2H_2O^{\bullet} + O^{\bullet} \rightarrow CH_2^{\bullet} + CO_2$	13	0.00

Table 1 (*Continued*)

	Reactions	log k_0 (s^{-1} or cm mol^{-1} s^{-1})	E (kJ/mol)
58	$C_2HO^{\bullet} + CH_3^{\bullet} \rightarrow C_2H_4 + CO$	12.3	0.00
59	$C_2HO^{\bullet} + O^{\bullet} \rightarrow H^{\bullet} + 2CO$	14.31	0.00
60	$H^{\bullet} + O_2 \rightarrow O^{\bullet} + OH^{\bullet}$	13.23	62.34
61	$O^{\bullet} + OH \rightarrow H^{\bullet} + O_2$	13.23	2.93
62	$H_2 + O^{\bullet} \rightarrow OH^{\bullet} + H^{\bullet}$	10.25	37.24
63	$H_2O_2 + OH^{\bullet} \rightarrow HO_2^{\bullet} + H_2O$	13	7.53
64	$HO_2^{\bullet} + H_2 \rightarrow H_2O_2 + H^{\bullet}$	6.2	0.00
65	$HO_2^{\bullet} + H^{\bullet} \rightarrow OH^{\bullet} + OH^{\bullet}$	14.18	4.18
Termination			
66	$C_2H_5^{\bullet} + C_2H_3^{\bullet} \rightarrow C_2H_4 + C_2H_4$	14.17	−10.88
67	$HO_2^{\bullet} + H^{\bullet} \rightarrow H_2 + O_2$	13.63	5.86
68	$HO_2^{\bullet} + HO_2^{\bullet} \rightarrow H_2O_2 + O_2$	12.3	0.00
69	$HO_2^{\bullet} + OH^{\bullet} \rightarrow H_2O + O_2$	13.7	4.18
70	$CH_3^{\bullet} + H^{\bullet} \rightarrow CH_4$	16.78	0.00
71	$CH_3^{\bullet} + CH_3^{\bullet} \rightarrow C_2H_6$	50.3	25.94
72	$CH_3^{\bullet} + CH_3^{\bullet} \rightarrow C_2H_4 + H_2$	16	133.89
73	$C_2H_3^{\bullet} + C_2H_3^{\bullet} \rightarrow C_2H_2 + C_2H_4$	13	0.00
74	$C_2H_5^{\bullet} + H^{\bullet} \rightarrow C_2H_4 + H_2$	13.65	0.00
75	$C_2H_5^{\bullet} + HO_2^{\bullet} \rightarrow C_2H_4 + H_2O_2$	13.48	4.18

tures, react mainly with ethane producing $C_2H_5^{\bullet}$ and CH_4. Methyl radicals react in parallel with oxygen to formaldehyde and a hydroxy radical and/or to the formaldehyde radical and $O^{\bullet}$.

The ethyl radical is also very important, since it is the main source for ethene production, reacting with molecular oxygen, $HO_2^{\bullet}$ and $H^{\bullet}$. The formation of $CH_3O^{\bullet}$ and formaldehyde leads to carbon oxides. The intermediately formed $CH_3O^{\bullet}$ reacts with oxygen generating $HCO^{\bullet}$, which in turn forms CO. In addition to the primary reactions, the model considers also secondary reactions especially those of ethene being critical for ethane oxidative dehydrogenation.

The model predictions for ethane and oxygen conversions agree well with the experimental values obtained at various temperatures with equimolar C_2H_6 and O_2 feed composition at 80 mbar ethane partial pressure (see Fig. 1). In addition to the total carbon oxides yields, the proposed kinetic scheme also accurately predicts the CO to CO_2 ratio. It should be noted that results obtained at lower oxygen partial pressures (48 and 16 mbar) are also satisfactorily modelled (not shown here).

4.2. Oxidative dehydrogenation of propane

Fig. 2 illustrates the conversion of propane and oxygen as a function of temperature obtained with equimolar feed composition at residence time 1.8 s. The conversion of propane increases rapidly with temperature reaching a value of 80% at 675 °C. Oxygen conversion, though lower than that of propane, increased also drastically with temperature illustrating the significant contribution of the oxidative dehydrogenation and of oxidation routes in general to the reaction network. The olefinic products observed were propene and ethene with yields up to 16% and 33%, respectively (Fig. 2). While ethene yield increased with temperature, propene yield had a maximum value indicating that propene undergoes secondary reactions at higher temperatures. Methane, a characteristic product of cracking reactions was produced in appreciable quantities. Carbon oxides (mainly CO) formation was mainly favored at temperatures higher than 650 °C with a maximum yield of 20%.

The structure of the model for the gas phase propane oxidative dehydrogenation was based on several studies about propane pyrolysis and oxidative dehydrogenation [9,12,14,15]. As in the case of ethane ODH, the propane ODH model includes the same categories of reactions (initiation, hydrogen atom abstraction, addition, decomposition reactions, etc.). After sensitivity analysis, the reaction model consists of 73 elementary reactions, in which 13 molecular compounds and 14 free radicals participate.

In brief, initiation reactions include reaction of propane with molecular oxygen producing $C_3H_7^{\bullet}$ and $HO_2^{\bullet}$, as well as cracking of propane to $CH_3^{\bullet}$ and $C_2H_5^{\bullet}$. In Table 2, the

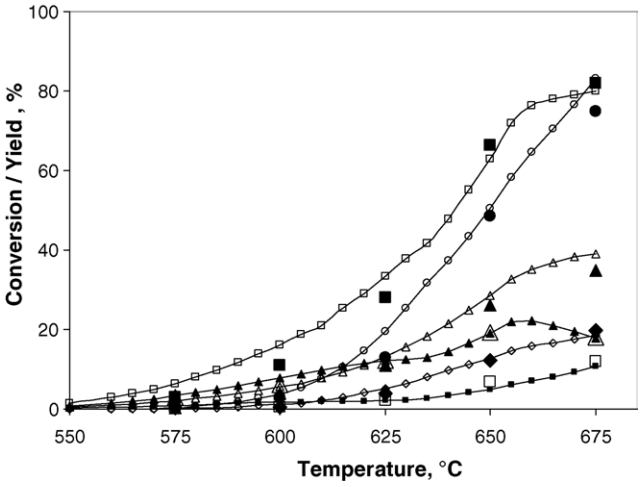

Fig. 2. Conversion and products yield vs. temperature in gas phase propane oxidative dehydrogenation (residence time = 1.8 s, $P_{C_3H_8} = P_{O_2} = 50$ mbar). C_3H_8: (■) experimental, (□) calculated; O_2: (●) experimental, (○) calculated; C_2H_4: (▲) experimental, (△) calculated; C_3H_6: (△) experimental, (▲) calculated; CH_4: (□) experimental, (■) calculated; COx: (◆) experimental, (◇) calculated.

Table 2
Elementary reactions and kinetic data for propane gas phase ODH [9,12,14,15]

	Reactions	$\log k_0$ (s^{-1} or cm mol^{-1} s^{-1})	E (kJ/mol)
Initiation			
1	$C_3H_8 \rightarrow CH_3^\bullet + C_2H_5$	15.97	325.93
2	$C_3H_8 + O_2 \rightarrow i\text{-}C_3H_7^\bullet + HO_2^\bullet$	12	199.58
3	$C_3H_8 + O_2 \rightarrow n\text{-}C_3H_7^\bullet + HO_2^\bullet$	12	199.58
Hydrogen atom abstraction			0.00
4	$CH_2^\bullet + H^\bullet \rightarrow CH^\bullet + H_2$	18	0.00
5	$C_3H_8 + H^\bullet \rightarrow i\text{-}C_3H_7^\bullet + H_2$	12.26	19.25
6	$C_3H_8 + H^\bullet \rightarrow n\text{-}C_3H_7^\bullet + H_2$	12.7	19.25
7	$C_3H_8 + CH_3^\bullet \rightarrow i\text{-}C_3H_7^\bullet + CH_4$	12.18	20.50
8	$C_3H_8 + CH_3^\bullet \rightarrow n\text{-}C_3H_7^\bullet + CH_4$	12.18	20.50
9	$CH_3^\bullet + H_2 \rightarrow CH_4 + H^\bullet$	13	47.70
10	$C_2H_5^\bullet + H_2 \rightarrow C_2H_6 + H^\bullet$	0	112.97
11	$CH_4 + i\text{-}C_3H_7^\bullet \rightarrow CH_3^\bullet + C_3H_8$	15.64	134.31
12	$CH_4 + n\text{-}C_3H_7^\bullet \rightarrow CH_3^\bullet + C_3H_8$	15.64	134.31
13	$C_3H_8 + C_2H_5^\bullet \rightarrow i\text{-}C_3H_7^\bullet + C_2H_6$	5.6	25.10
14	$C_3H_8 + C_2H_5^\bullet \rightarrow n\text{-}C_3H_7^\bullet + C_2H_6$	5.6	25.10
15	$C_3H_8 + O^\bullet \rightarrow i\text{-}C_3H_7^\bullet + OH^\bullet$	6.7	12.55
16	$C_3H_8 + O^\bullet \rightarrow n\text{-}C_3H_7^\bullet + OH^\bullet$	6.7	12.55
17	$CH_3^\bullet + OH^\bullet \rightarrow CH_4 + O^\bullet$	11.43	27.61
18	$C_3H_8 + OH^\bullet \rightarrow i\text{-}C_3H_7^\bullet + H_2O$	6	40.17
19	$C_3H_8 + OH^\bullet \rightarrow n\text{-}C_3H_7^\bullet + H_2O$	6	40.17
20	$CH_3^\bullet + HO_2^\bullet \rightarrow CH_4 + O_2$	11.65	−6.69
21	$C_2H_4 + HO_2^\bullet \rightarrow C_2H_5^\bullet + O_2$	11.12	57.32
22	$C_3H_8 + HO_2^\bullet \rightarrow i\text{-}C_3H_7^\bullet + H_2O_2$	7	50.21
23	$C_3H_8 + HO_2^\bullet \rightarrow n\text{-}C_3H_7^\bullet + H_2O_2$	7	50.21
24	$C_2H_3^\bullet + O_2 \rightarrow C_2H_2 + HO_2^\bullet$	11.1	0.00
25	$C_2H_5^\bullet + O_2 \rightarrow C_2H_4 + HO_2^\bullet$	6	0.00
26	$i\text{-}C_3H_7^\bullet + O_2^\bullet \rightarrow C_3H_6 + HO_2^\bullet$	6	0.00
27	$n\text{-}C_3H_7^\bullet + O_2 \rightarrow C_3H_6 + HO_2^\bullet$	6	0.00
28	$CH_3^\bullet + H_2O \rightarrow CH_4 + OH^\bullet$	2.76	69.87
29	$CH_3^\bullet + H_2O_2 \rightarrow CH_4 + HO_2^\bullet$	12.02	6.28
30	$i\text{-}C_3H_7^\bullet + H_2O_2 \rightarrow C_3H_8 + HO_2^\bullet$	12.01	35.15
31	$n\text{-}C_3H_7^\bullet H_2O_2 \rightarrow C_3H_8 + HO_2^\bullet$	12.01	35.15
Addition			0.00
32	$CH_2^\bullet + CO \rightarrow C_2H_2O^\bullet$	10.66	0.00
33	$C_2H_2 + C_2H_2^\bullet \rightarrow C_4H_3^\bullet + H^\bullet$	13	188.28
34	$C_2H_4 + C_2H_4 \rightarrow C_2H_5^\bullet + C_2H_3^\bullet$	14.3	268.61
35	$C_2H_2 + O_2 \rightarrow HCO^\bullet + HCO^\bullet$	12.6	117.15
36	$H_2O + O_2 \rightarrow HO_2^\bullet + OH^\bullet$	14.8	309.20
Decomposition			0.00
37	$C_2H_4 \rightarrow C_2H_2 + H_2$	16.97	323.00
38	$i\text{-}C_3H_7^\bullet \rightarrow C_3H_6 + H^\bullet$	10.56	133.47
39	$n\text{-}C_3H_7^\bullet \rightarrow C_2H_4 + CH_3^\bullet$	10.58	133.47
40	$C_4H_3^\bullet + H^\bullet \rightarrow C_2H_2 + C_2H_2$	13.18	0.00
41	$C_2H_2O \rightarrow CO + CH_2^\bullet$	15.6	248.11
42	$HO_2^\bullet \rightarrow O_2 + H^\bullet$	15.36	192.05
43	$H_2O \rightarrow OH^\bullet + H^\bullet$	16.34	439.32
44	$H_2O_2 \rightarrow OH^\bullet + OH^\bullet$	6	46.02
Carbon oxides formation			0.00
45	$CH_3^\bullet + O_2 \rightarrow CH_2O + OH^\bullet$	10.2	0.00
46	$CH_3^\bullet + CH_2O \rightarrow CH_4 + HCO^\bullet$	−7	8.37
47	$CH_2^\bullet + O_2 \rightarrow HCO^\bullet + OH^\bullet$	14	15.48
48	$CH_2^\bullet + O_2 \rightarrow CO_2 + H_2$	12.9	2.93
49	$CH^\bullet + O_2 \rightarrow CO + OH^\bullet$	11.13	107.53
50	$C_2H_2 + OH^\bullet \rightarrow C_2H_2O^\bullet + H^\bullet$	11.51	0.84
51	$C_2H_5^\bullet + CH_2O \rightarrow C_3H_6 + OH^\bullet$	13.66	72.80
52	$C_3H_6 + O^\bullet \rightarrow C_2H_5^\bullet + HCO^\bullet$	12.5	8.37
53	$C_2H_2O^\bullet + O^\bullet \rightarrow CH_2^\bullet + CO_2$	17	0.00
54	$CH_2O + O_2 \rightarrow HCO^\bullet + HO_2^\bullet$	12	62.76
55	$CH_2O + O^\bullet \rightarrow HCO^\bullet + OH^\bullet$	13.26	12.97
56	$HCO^\bullet + HO_2^\bullet \rightarrow CH_2O + O_2$	14	12.55
57	$HCO^\bullet + O_2 \rightarrow CO + HO_2^\bullet$	10	0.00

Table 2 (*Continued*)

	Reactions	log k_0 (s^{-1} or cm mol^{-1} s^{-1})	E (kJ/mol)
58	$HCO^{\bullet} + OH^{\bullet} \rightarrow CH_2O + O^{\bullet}$	12.24	71.96
59	$CO + OH^{\bullet} \rightarrow CO_2 + H^{\bullet}$	3.18	−3.35
60	$CO_2 + H^{\bullet} \rightarrow CO + H^{\bullet}$	9.23	90.37
61	$CO_2 + OH^{\bullet} \rightarrow HO_2^{\bullet} + CO$	15.23	357.31
62	$CO_2 + O^{\bullet} \rightarrow CO + O_2$	12.44	183.26
63	$CO + O_2 \rightarrow CO_2 + O^{\bullet}$	11.5	157.32
64	$H^{\bullet} + O_2 \rightarrow O^{\bullet} + OH^{\bullet}$	14.34	70.29
65	$O^{\bullet} + OH^{\bullet} \rightarrow H^{\bullet} + O_2$	17.24	2.93
66	$H_2O_2 + OH^{\bullet} \rightarrow HO_2^{\bullet} + H_2O$	13	7.53
Termination			0.00
67	$H^{\bullet} + OH^{\bullet} \rightarrow H_2O$	22.34	0.00
68	$HO_2^{\bullet} + OH^{\bullet} \rightarrow H_2O + O_2$	13.7	4.18
69	$CH_3^{\bullet} + C_2H_5^{\bullet} \rightarrow C_3H_8$	12.62	0.00
70	$i\text{-}C_3H_7^{\bullet} + HO_2^{\bullet} \rightarrow C_3H_8 + O_2$	12.31	−15.48
71	$n\text{-}C_3H_7^{\bullet} + HO_2^{\bullet} \rightarrow C_3H_8 + O_2$	12.31	−15.48
72	$i\text{-}C_3H_7^{\bullet} + CH_3^{\bullet} \rightarrow CH_4 + C_3H_6$	12.1	0.00
73	$n\text{-}C_3H_7^{\bullet} + CH_3^{\bullet} \rightarrow CH_4 + C_3H_6$	12.1	0.00

reactions and their kinetic data are presented. As with ethane initiation reactions, the contribution of the oxidative route in this step is quite important as depicted from the significantly lower activation energy of reactions (2) and (3) compared to the pyrolysis route (1).

Radicals formed via initiation steps cause chain reactions. The ethyl radical reacts with propane to a propyl radical and ethane. Propane reacts also with $CH_3^{\bullet}$ generating CH_4 and $C_3H_7^{\bullet}$. The propyl radical is the main source for propene production. It reacts with oxygen to the desired C_3H_6 and $HO_2^{\bullet}$ and cracks to C_3H_6 and $H^{\bullet}$ and to C_2H_4 and $CH_3^{\bullet}$. Methyl radical reactions lead to CH_4 and CH_2O formation. CH_2O is responsible for carbon oxides formation through $HCO^{\bullet}$.

The results from the experiments (conversions and product yields) and the calculated results from the propane ODH model are presented in Fig. 2. The reaction network used in the model adequately describes the experimental results obtained from 575 to 675 °C at residence time 1.8 s. The agreement between experimental and calculated values is also satisfactory for results obtained at lower residence times (not shown). The small deviations between experimental and calculated results observed are speculated to be due to the absence of surface reactions with the reactor walls and the values of the kinetic parameters taken from literature.

4.3. Relevance of gas phase to catalytic kinetic mechanisms

Even though the proposed gas phase kinetic schemes for ethane and propane cannot be directly applied in the presence of catalysts, they can be used in combination with heterogeneous reaction scheme to describe performance of the catalysts at high temperature. The contribution of homogeneous radical reactions in alkane oxidation can in general be neglected for reducible metal oxide catalysts, which typically operate at lower temperatures. On the contrary, homogeneous gas phase reactions may play fundamental role when operation is carried out at higher temperatures, typical of the non-redox type catalysts [3,16]. There are certain similarities and common intermediates between the homogeneous and heterogeneous reaction schemes. In the presence of a catalyst, alkyl (or alkoxy) radicals are formed by the homolytic C–H bond cleavage assisted by the surface oxidizing center [O] on the surface. These species are transformed on the surface via β-elimination to the corresponding alkene or undergo further attack by oxygen species to formates, which are considered as the precursors for COx formation. Transformation of alkyl species may proceed in the gas phase via chain radicals reactions over non-redox catalysts. In the proposed gas phase model the formation of the alkyl species is considered as the most important kinetically relevant step determining the conversion of the alkanes. Hydrogen abstraction reactions contribute significantly to the selectivity of alkenes while COx formation proceeds via formates. Literature data about the intermediates formed during heterogeneous–homogeneous alkane ODH are rather limited. Zerkle et al. [17] claimed that the dominant homogeneous reaction in ethane catalytic oxidation is the formation of ethyl radical, which decomposes to form ethylene. Common intermediates and relative importance of the various homogeneous and heterogeneous steps are systematically investigated in the work of Vislovskiy et al. [8].

Worth noting that even though certain routes are common in homogeneous and heterogeneous schemes, the distribution of the products is quite different due to the selective enhancement of specific reaction rates (like the COx formation) on the catalyst surface.

5. Conclusions

The present results demonstrate the importance of homogeneous gas phase reactions in oxidative dehydrogenation of C_2–C_3 alkanes. In general, at temperatures higher than 600 °C ethane and propane are selectively converted to the corresponding alkenes. Ethene yield as high as 56% can be achieved at 650 °C. At the same temperature propane oxidatively cracks

and dehydrogenates producing total olefins up to 40%. Mechanistic kinetic models were developed for ethane and propane gas phase oxidative dehydrogenation using existing information on the elementary reactions. The set of the elementary reactions selected, describe the conversion of alkanes and the yield of the products at various temperatures and residence times. In general, gas phase oxidative dehydrogenation leads to high yields of olefins and the kinetic models developed can be used as a basis for modelling similar reactions also in the presence of catalysts active at high temperatures by coupling the reactions occurring at the surface and in the homogeneous gas phase. The data suggest that with ethane the oxidative route seems to dominate under all conditions. With propane, true oxidative dehydrogenation occurs at relatively low temperatures while at high temperature combustion and pyrolysis routes are predominant.

Acknowledgment

Greek–German bilateral program is acknowledged for the financial support.

References

[1] G. Centi, F. Cavani, F. Trifiro, Selective Oxidation by Heterogeneous Catalysis, Kluwer Academic–Plenum Publishers, New York, 2001 .
[2] M. Yu Sinev, J. Catal. 216 (2003) 468.
[3] L. Leveles, K. Seshan, J.A. Lercher, J.L. Lefferts, J. Catal. 218 (2003) 296.
[4] R. Burch, E.M. Grabb, Appl. Catal. A 97 (1993) 49.
[5] S.A.R. Mulla, O.V. Buyevskaya, M. Baerns, Appl. Catal. A 226 (2002) 73.
[6] A. Beretta, P. Forzatti, E. Ranzi, J. Catal. 184 (1999) 469.
[7] A.A. Lemonidou, A.E. Stambouli, Appl. Catal. A 171 (1998) 325.
[8] V.P. Vislovskiy, T.E. Suleimanov, M. Yu Sinev, P. Yu, L. Tulenin, V. Ya Margolis, Cortes Corberan Catal. Today 61 (2000) 287.
[9] K.T. Nguyen, H.H. Kung, Ind. Eng. Chem. Res. 30 (1991) 352.
[10] Y. Hidaka, K. Sato, H. Hoshikawa, T. Noshimori, R. Takahashi, H. Tanaka, K. Inami, N. Ito, J. Combus. Flame 120 (2000) 245.
[11] K. Sato, Y. Hidaka, J. Combus. Flame 122 (2000) 291.
[12] D. Patel, Ph.D. Thesis, Northwestern University, 1988.
[13] C.K. Westbrook, W.J. Pitz, Combus. Sci. Technol. 37 (1984) 117.
[14] S.K. Layokun, Ind. Eng. Chem. Process Des. Dev. 18 (1979) 241.
[15] R.P. O'Connor, L.D. Schmidt, AlChE J. 48 (2002) 1241.
[16] F. Cavani, F. Trifiro, Catal. Today 51 (1999) 561.
[17] D.K. Zerkle, M.D. Allendorf, M. Wolf, O. Deutschmann, J. Catal. 196 (2000) 18.